Journal of Electroanalytical Chemistry 778 (2016) 98–102

Contents lists available at ScienceDirect

Journal of Electroanalytical Chemistry

journal homepage: www.elsevier.com/locate/jelechem

Electrochemical synthesis of Rh-Pd bimetallic nanoparticles onto a glassy carbon surface

A.L. Querejeta, M.C. del Barrio, S.G. García *,[1]

Instituto de Ing. Electroquímica y Corrosión (INIEC), Departamento de Ingeniería Química, Universidad Nacional del Sur, Avda. Alem 1253, 8000 Bahía Blanca, Argentina

ARTICLE INFO

Article history:
Received 3 May 2016
Received in revised form 22 July 2016
Accepted 25 July 2016
Available online 26 July 2016

Keywords:
Bimetallic particles
Rhodium
Palladium
Electrodeposition

ABSTRACT

Rh-Pd bimetallic nanoparticles were prepared successfully by sequential electrodeposition on a glassy carbon (GC) substrate using single potentiostatic pulses. The generated particles were characterized by ex-situ atomic force microscopy (AFM) and X-ray photoelectron spectroscopy (XPS). Initially, AFM images evidenced hemispherical-shaped Pd crystals distributed preferably over the GC surface defects. Size diversity of the formed deposits indicates a progressive nucleation mechanism with a three-dimensional growth. Subsequent Rh deposition does not introduce significant morphological changes. Voltammetric results suggested that Rh is deposited over Pd nanocrystals forming a core-shell type structure. XPS analysis confirms that Pd and Rh are present on the surface, both as metal and as oxide compounds. The relative amount of Rh greater than that of Pd, corroborates that Rh atoms were preferentially at the surface of the bimetallic particles as a shell over the Pd core. The electrocatalytic effect of the Rh-Pd/CV modified electrode was evaluated qualitatively for the hydrogen evolution reaction.

1. Introduction

The electrochemical formation of metal particles on an inert substrate has received considerable attention in recent times, due to the great interest in developing new materials that act as catalysts for certain reactions of technological importance such as the hydrogen electrode reaction (HER). In addition, bimetallic systems may improve the properties of each metal due to the synergistic effect of its components, being the study of these systems an attractive area of research within nanoelectrochemistry (especially in electrocatalysis and sensors), by exhibiting particular optical, catalytic and magnetic properties [1–4].

Metals belonging to the Pt group, such as Rh and Pd, are known to be some of the best catalytic metals for the HER [5,6], and the formation of disperse nanoparticles of both metals is an important task to develop new materials with high electrocatalytic activity and low cost. The early stages of the electrodeposition of Pd onto glassy carbon (GC) substrate was studied by Alvarez and Salinas [2], and they demonstrated that the kinetics of this process could be described by a model involving progressive nucleation on active sites and diffusion-controlled 3D growth, which was corroborated with AFM images. In the case of Rh, the metal electrodeposition on a carbon disk electrode was investigated in chloride [7] and sulphate [8] solutions. The authors reported that although the Rh(III) exists as a mixture of aquo/chloro complexes, only a single reduction peak for all the Rh(III) species was observed in the cyclic voltammograms. The corresponding anodic peaks related to Rh stripping were not evidenced because this metal forms a passive oxide layer that prevents its dissolution. Moreover, as in the case of Pd, the Rh electrodeposition follows a progressive nucleation mechanism with a 3D growth under diffusion control although it was demonstrated by Schulz et al. [9] that this phenomenon involved a combination of several nucleation processes if the GC electrode was electrochemically pretreated: two-dimensional (2D) progressive nucleation, which transforms to 2D instantaneous nucleation at more cathodic potentials, followed by three-dimensional (3D) nucleation with diffusion controlled growth. Considering the previous studies, the Rh-Pd bimetallic particles appear as an interesting system to be considered and its preparation by electrodeposition has not been practically analyzed so far. Recently, Rh-Pd particles were electrodeposited on GC and indium tin oxide (ITO) electrode surfaces by cyclic voltammetry from an electrolyte containing both metallic cations [1]. SEM images of the Rh-Pd deposits obtained on ITO have an average size range of 30-200 nm and were found to be useful for the detection of H_2O_2, while those deposited onto GC were not morphologically characterized.

Considering the limited information about the electrochemical formation of this bimetallic system, the aim of this paper is to report the preparation of Rh-Pd bimetallic particles on GC electrodes, by sequential electrodeposition of both metals from solutions containing the corresponding metal ions, using conventional electrochemical techniques. Ex-situ AFM and XPS analysis were employed for their morphological and elemental characterization, respectively. The catalytic effect for the hydrogen evolution reaction was qualitatively analyzed by cyclic voltammetry.

* Corresponding author.
E-mail address: sgarcia@criba.edu.ar (S.G. García).
[1] ISE Member.

http://dx.doi.org/10.1016/j.jelechem.2016.07.035
1572-6657/

2. Experimental

The formation of Rh-Pd nanostructures on GC was performed by sequential deposition from 1 mM $PdCl_2$ + 24 mM HCl + 0.1 M Na_2SO_4 (pH = 2.6) and 5 mM Na_3RhCl_6 + 0.5 M NaCl (pH = 3.37) aqueous solutions, for Pd and Rh respectively. Electrolytic solutions were prepared with pro-analysis grade reagents (Merck, Darmstadt) and tri-distilled water and deaerated by bubbling of nitrogen gas prior to each experiment.

Electrochemical measurements were carried out at T = 298 K in a conventional three-electrode electrochemical cell. A GC sheet disposed into a Teflon holder, with an exposed area of 0.21 cm^2, was used as working electrode. The electrode surface was mechanically polished with progressively finer emery paper and subsequently with 0.3 μm particle size Al_2O_3 powder, until a mirror like finished surface was obtained. Finally, it was thoroughly washed with tri-distilled water. A Pt sheet and a Hg/Hg_2Cl_2/KCl saturated calomel electrode (SCE) were used as counter and reference-electrodes, respectively. All potentials in this study are referred to the SCE.

Conventional electrochemical techniques were carried out with a potentiostat/galvanostat EG&G Princeton Applied Research Model 273A. A standard Nanoscope III equipment (Digital Instruments, Santa Barbara, CA, USA) was used for the ex-situ AFM studies, operated in contact mode, employing silicon nitride probes (5–40 nm radius) (Veeco probes). XPS analysis were performed by using a multitechnique system (SPECS) equipped with a dual Ag/Al X-ray monochromatic source and a hemispherical PHOIBOS 150 analyzer operating in the fixed analyzer transmission (FAT) mode. The spectra were obtained with pass energy of 30 eV and an Al monochromatic anode was operated at 300 W. The working pressure in the analyzing chamber was $<2 \times 10^{-9}$ mbar. The data treatment was performed with the Casa XPS program (Casa Software Ltd., UK).

3. Results and discussion

Initially, the electrodeposition of Pd on GC substrates was evaluated qualitatively by cyclic voltammetry from solutions containing the Pd^{2+} cations. The voltammetric results showed the response of a 3D nucleation and growth process controlled by diffusion (Fig. 1), which are in agreement with those reported by other authors [2]. The cyclic voltammogram for the system GC/1 mM $PdCl_2$ + 24 mM HCl + 0.1 M Na_2SO_4 shows, during the cathodic scan, a well-defined peak (I) at $E_{p,I}$ = 0.190 V, corresponding to the nucleation and growth of Pd on GC. At more negative potential values, two peaks are evidenced related to the hydrogen adsorption (II) and hydrogen evolution (III) processes. During the reverse scan, the peaks corresponding to the hydrogen oxidation (IV) and desorption (V) phenomena, are observed. The current increase from E ~ 0.5 V (denoted as VI), is attributed to the dissolution of the Pd deposits previously formed.

In order to obtain structural information of the metal deposits, Pd nanocrystals were electrodeposited onto a polished GC electrode applying a simple potentiostatic pulse, from E_0 = 0.7 V to E_1 = 0.215 V, during 15 s, and characterized by ex-situ AFM. Fig. 2 shows a representative AFM image of the Pd crystals with the corresponding particle size distribution. These crystals are distributed randomly on the GC substrate, preferably over the surface defects, presenting a significant density of nuclei. The size diversity of the hemispherical-shaped Pd particles (ranging from 114 nm to 295 nm approximately) indicates that the electrodeposition process of Pd on GC follows a progressive nucleation mechanism with a three-dimensional (3D) growth, as it was previously reported by Alvarez and Salinas [2].

After characterizing the Pd/GC system, it was proceeded to analyze the electrodeposition of Rh on Pd nanoparticles (NPs) supported on GC, immersing the modified substrate in the solution containing Rh^{3+} ions. Fig. 3 shows the voltammetric response of the system GC/Pd(NPs)/Rh^{3+}, where the cyclic voltammogram for the system GC/Rh^{3+}, was also included for comparison. It is observed that the cathodic and anodic current peaks associated with processes related to the H_2 reaction are very similar for both surfaces, i.e. GC and GC/Pd(NPs). Conversely, the Rh nucleation and growth onto the GC/Pd(NPs) modified

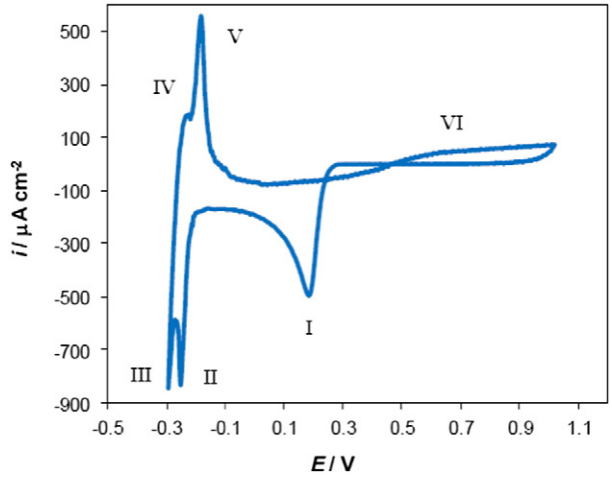

Fig. 1. Cyclic voltammogram for the system GC/1 mM $PdCl_2$ + 24 mM HCl + 0.1 M Na_2SO_4. |dE/dt| = 10 mV s^{-1}.

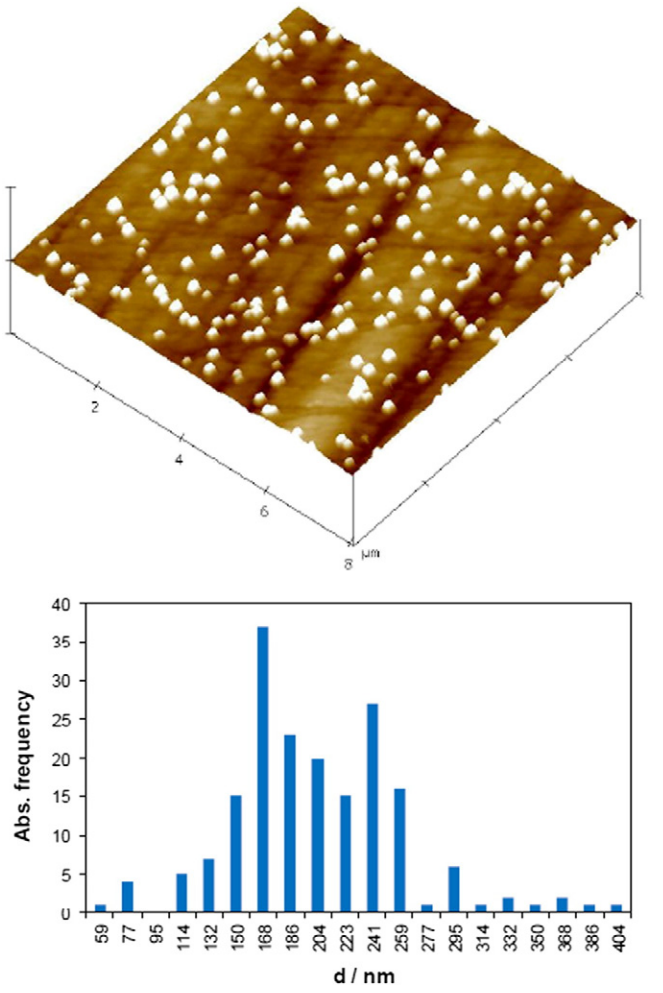

Fig. 2. Ex-situ AFM image of Pd nanocrystals on a GC electrode obtained by a simple potentiostatic pulse (E_0 = 0.7 V, E_1 = 0.215 V, t_1 = 15 s), and the corresponding size distribution.

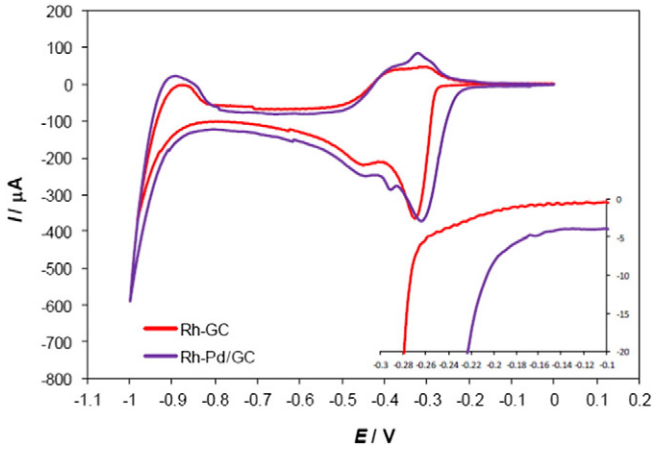

Fig. 3. Cyclic voltammograms for GC and Pd(NPs)/GC substrates in a 5 mM Na_3RhCl_6 + 0.5 M NaCl solution. $|dE/dt| = 10$ mV s^{-1}.

electrode (well-defined peak denoted as I, at $E_{p,I} = -0.320$ V) occurs at lower potential values, approximately 100 mV before, as it is more clearly observed in the inset of the figure, indicating that the presence of Pd crystals remarkably promotes Rh nucleation. From the voltammetric profile, a cathodic feature was observed before the hydrogen evolution reaction (III), which starts at E ~ −0.8 V. The smaller peak (denoted as II), observed $E_{p,II} = -0.440$ V, and the anodic peak V recorded on the reverse scan ($E_{p,V} = -0.350$ V) were attributed to the hydrogen adsorption/desorption onto the freshly deposited Rh particles, respectively [7]. The first anodic current peak at the most negative potential, denoted as IV, corresponds to the hydrogen oxidation process. No anodic peaks related to the stripping of Rh are present because this metal does not dissolve anodically within the potential range considered.

On the other hand, a new cathodic peak was also observed in the cyclic voltammogram, located at E = −0.380 V, which could be associated with hydrogen adsorption and/or evolution processes on the exposed Pd nanoparticles not covered with Rh deposits. During the positive-going sweep, another peak is evidenced at E = −0.330 V, related to the corresponding hydrogen oxidation and/or desorption phenomena on the Pd deposits. Nevertheless, further studies are in progress to confirm this assumption.

Considering these previous results, it was proceeded to generate the bimetallic structure by the deposition of Rh on the previously deposited Pd crystals by choosing adequate potentiostatic pulse conditions. The synthesis of Rh-Pd bimetallic particles was then carried out, immersing the Pd(NPs)/GC modified substrate in the solution containing Rh^{3+} ions, and applying a simple potential step from $E_0 = 0$ V, to $E_1 = -0.16$ V during 150 s. The potential E_1 was selected at a value where the current, according to the cyclic voltammogram in Fig. 3, begins to increase and it is practically negligible for the system Rh/GC, thus discarding the Rh deposition on the GC substrate free of Pd deposits. In addition, it is worth mentioning that this potential step was previously tested on a polished GC electrode, obtaining a record with very low currents. Furthermore, it was confirmed by ex-situ AFM that no Rh particles were evidenced on the GC surface in the selected potential value (image not shown). By this way, it was assured that the Rh is selectively deposited on the previously formed Pd nanoparticles supported on GC, generating probably Pd-core-Rh-shell structure.

Bimetallic Rh-Pd crystals prepared by applying the routine previously described were morphologically characterized by ex-situ AFM (Fig. 4). The AFM image consists of well-dispersed hemispherical Rh-Pd nanoparticles. The observed morphology is very similar to that recorded for Pd crystals on GC (cf. Fig. 2), indicating that Rh deposits do not introduce significant morphological changes on the electrode surface. This is a first indication of the formation of a core-shell type structure, where

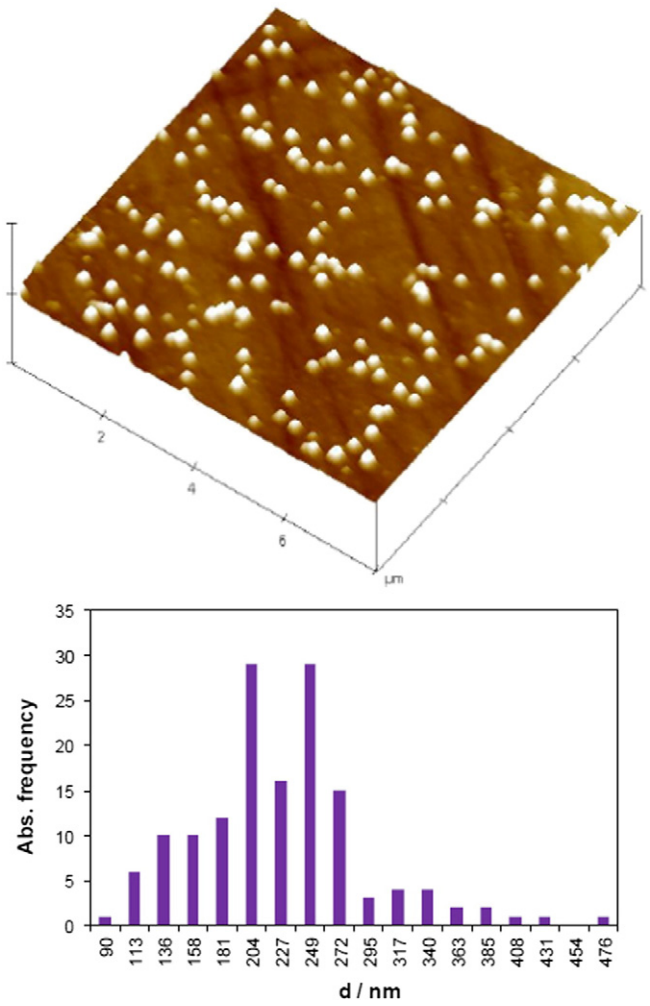

Fig. 4. Ex-situ AFM image of Pd-Rh nanocrystals electrodeposited on a GC electrode and the corresponding size distribution.

Rh is selectively deposited on Pd crystals previously generated on GC. A statistic analysis of the image yielded a particle size distribution with diameters ranging from 113 to 385 nm approximately.

Voltammetric measurements were then carried out in a 0.5 M H_2SO_4 solution at a scan rate $|dE/dt| = 100$ mV s^{-1}, to characterize electrochemically the Rh-Pd modified GC electrode. Fig. 5 shows the voltammetric response, which is similar to those obtained for metallic rhodium [10] and nanostructured Rh electrodes generated by sputtering on a GC substrate [11]. The cathodic current peaks II and III are referred to the hydrogen adsorption and evolution processes, respectively. At potential values more positive than those related to the hydrogen process, a current peak (I), related to the reduction of Rh surface oxides, is evidenced at E = 0.20 V. During the positive scan, the two first anodic features, i.e. peaks IV and V, are attributed to the hydrogen oxidation and desorption phenomena. At more positive potentials, a current increase at E > 0.6 V, corresponds to the Rh oxide formation region (VI). The behavior observed for the Rh-Pd/GC system suggests that Rh atoms are preferentially at the surface of the bimetallic particles as a shell over a Pd core.

In order to corroborate this assumption, the physicochemical characterization of the bimetallic particles was carried out by XPS analysis (Figs. 6 and 7). The elements present in the sample (C, O, Pd and Rh) are clearly identified in Fig. 6. Fig. 7 exhibits the spectra in the 325–350 eV (Fig. 7a) and 300–325 eV (Fig. 7b) ranges, corresponding to the Pd 3d and Rh 3d regions, respectively. The deconvolution of the peaks is also shown (gray lines). In both cases, the curve-fitting involved

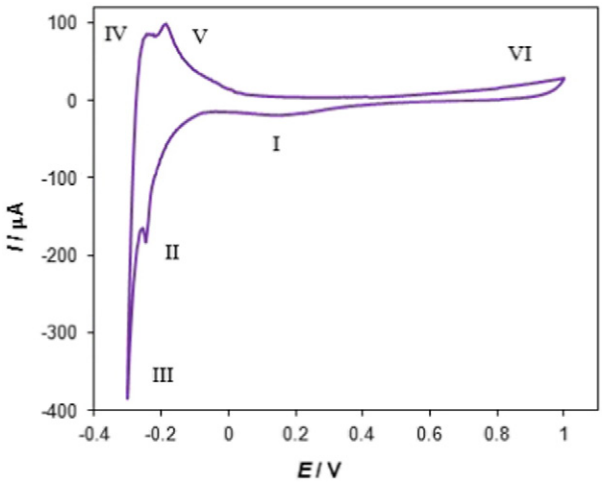

Fig. 5. Cyclic voltammogram for the Rh-Pd/GC electrode in a 0.5 M H_2SO_4 solution. |dE/dt| = 100 mV s^{-1}.

two separate doublets to accurately reproduce the shape of the spectrum, the one associated with binding energies corresponding to the metallic state and the second doublet in the envelope, at higher binding energies, consistent with the metal present in a higher oxidation state. The binding energies corresponding to the reduced and oxidized species for Rh and Pd are in agreement with the values reported in the literature [12–14]. From the peaks analysis, it is possible to determine that the relation Rh/Pd is 2.70. Although a Rh-Pd surface alloy could not be completely discarded, the relative amount of Rh greater than that of Pd, together with the voltammetric results shown above, and the lack of morphological changes, suggest that the Rh is deposited over the Pd nanocrystals supported on GC, forming a core-shell type structure.

Finally, the catalytic effect of the Rh-Pd/GC and Pd/GC systems were evaluated qualitatively for the hydrogen evolution reaction in a 0.5 M H_2SO_4 solution, at a scan rate of 10 mV s^{-1}, as it is shown in Fig. 8. In this figure, the behavior of the substrate free of deposits is also added. As expected, Pd(NPs)/GC and Rh-Pd(NPs)/GC modified electrodes decreases the overpotential required to produce the HER as compared to the GC substrate. Particularly, the surface of Rh-Pd(NPs)/GC facilitated the evolution of hydrogen since the onset potential of HER occurs at about −0.3 V, and is indicated by an increase of the cathodic current. It can be seen that the presence of Rh enhances the catalytic effect for the HER compared to that of the GC electrode modified with Pd crystals. Taking into account a theoretical analysis reported for hydrogen adsorption on Rh/Pd(111) [15], this fact could be associated with geometric and electronic effects induced by the Pd nanoparticles, which act as

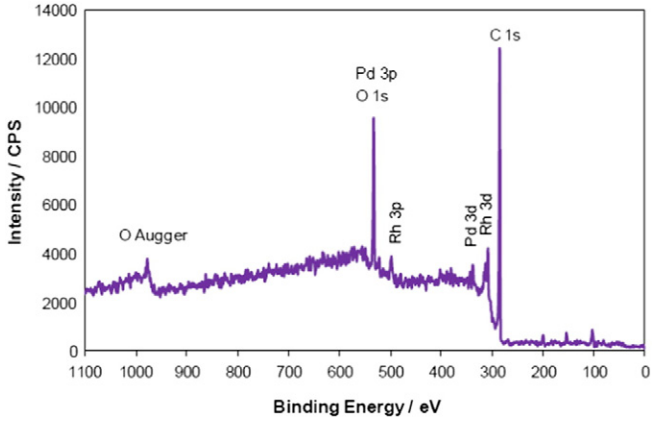

Fig. 6. XPS spectrum of the Rh-Pd nanostructures supported on a GC substrate.

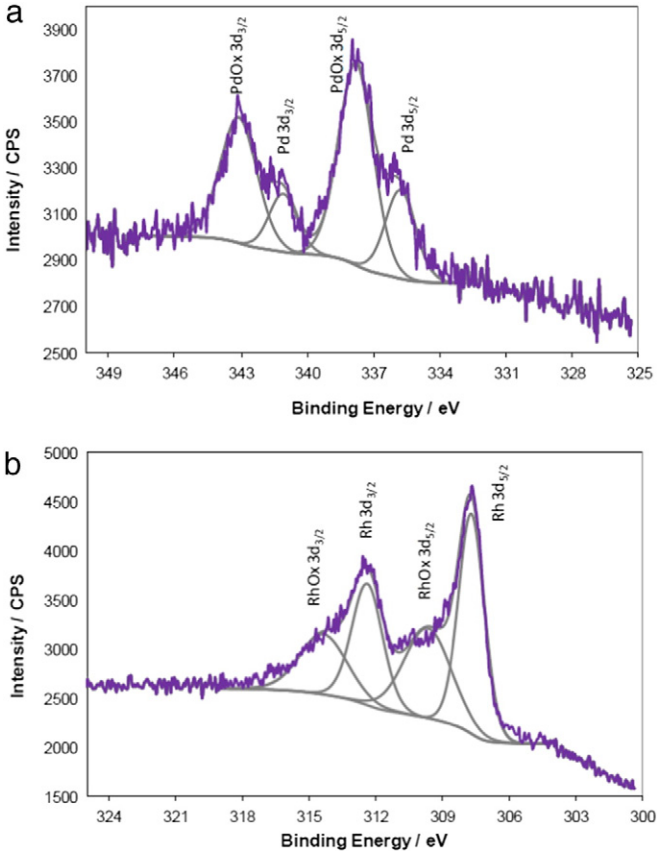

Fig. 7. XPS spectra of the a) Pd 3d and b) Rh 3d regions, and the associated deconvolution peaks, for the Rh-Pd particles supported on a GC electrode.

substrates for Rh deposits, favoring the hydrogen adsorption (intermediate species in the HER) on Rh nanoparticles. Thus, a synergistic effect between the two metals, Pd and Rh, which produces a considerable increase in current at more positive potential values, is verified. A kinetic study for this system involving the Tafel–Heyrovsky–Volmer mechanism is now in progress.

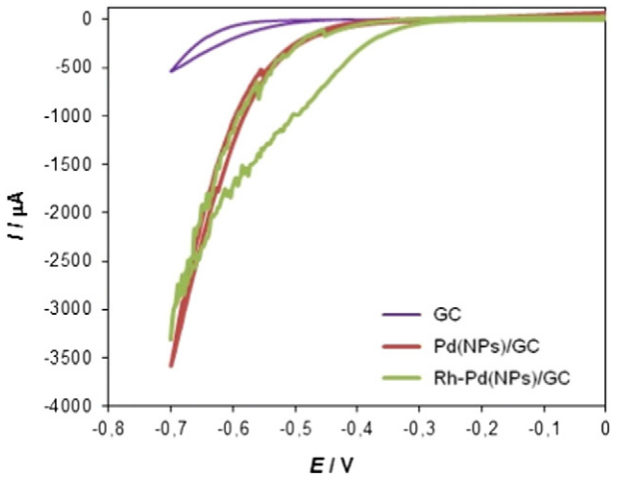

Fig. 8. Cyclic voltammograms of the analyzed systems for the HER in a 0.5 M H_2SO_4 solution. |dE/dt| = 10 mV s^{-1}.

4. Conclusions

The formation of Rh-Pd nanoparticles was achieved successfully by sequential electrodeposition of the metal components on GC substrates. AFM images show hemispherical Pd crystals, distributed preferably on the surface defects of the substrate. Size diversity indicates that the electrodeposition process of Pd on GC follows a progressive nucleation mechanism with a three-dimensional growth. Subsequent Rh deposition does not introduce significant morphological changes on the Pd(NPs)/GC modified electrode, suggesting that Rh is selectively deposited on Pd crystals previously generated on GC. XPS analysis confirms that Pd and Rh are present on the surface, both as metal and as oxide compounds. Although a surface alloy could not be completely discarded, the relative amount of Rh greater than that of Pd, together with the voltammetric results and the AFM images, suggested that the Rh is deposited over the Pd nanocrystals forming a core-shell type structure. From the qualitative analysis of the electrocatalytic behavior for the HER, it was demonstrated a higher catalytic effect of the bimetallic Rh-Pd particles than that of the individual components.

Acknowledgements

The authors wish to thank the Universidad Nacional del Sur (PGI-UNS 24/M128) and CONICET (PIP-0853), Argentina, for financial support of this work. A. L. Querejeta acknowledges a fellowship granted by CONICET.

References

[1] M. Rajkumar, S. Thiagarajan, S.-M. Chen, Electrochemical fabrication of Rh–Pd particles and electrocatalytic applications, J. Appl. Electrochem. 41 (2011) 663–668.
[2] A. Alvarez, D.R. Salinas, Formation of Cu/Pd bimetallic crystals by electrochemical deposition, Electrochim. Acta 55 (2010) 3714–3720.
[3] M. Smiljanic, Z. Rakocevic, A. Maksic, S. Strbac, Hydrogen evolution reaction on platinum catalyzed by palladium and rhodium nanoislands, Electrochim. Acta 117 (2014) 336–343.
[4] B.J. Murray, E.C. Walter, R.M. Penner, Amine vapor sensing with silver mesowires, Nano Lett. 4 (2004) 665–670.
[5] S. Trasatti, Work function, electronegativity and electrochemical behaviour of metals: electrolytic hydrogen evolution in acid solutions, J. Electroanal. Chem. 39 (1972) 163–184.
[6] L.A. Kibler, Hydrogen electrocatalysis, ChemPhysChem 7 (2006) 985–991.
[7] D. Pletcher, R.I. Urbina, Electrodeposition of rhodium. Part 1. Chloride solutions, J. Electroanal. Chem. 421 (1997) 137–144.
[8] D. Pletcher, R.I. Urbina, Electrodeposition of rhodium. Part 2. Sulfate solutions, J. Electroanal. Chem. 421 (1997) 145–151.
[9] E.N. Schulz, D.R. Salinas, S.G. García, Electrodeposition of rhodium onto a pre-treated glassy carbon surface, Electrochem. Commun. 12 (2010) 583–586.
[10] B. Łosiewicz, B. Jurczakowski, A. Lasia, Kinetics of hydrogen underpotential deposition at polycrystalline rhodium in acidic solutions, Electrochim. Acta 56 (2011) 5746–5753.
[11] M.A. Montero, J.L. Fernández, M.R. Gennero de Chialvo, A.C. Chialvo, Characterization and kinetic study of a nanostructured rhodium electrode for the hydrogen oxidation reaction, J. Power Sources 254 (2014) 218–223.
[12] M.C. Militello, S.J. Simko, Elemental palladium by XPS, Surf. Sci. Spectra 3 (1994) 387–394.
[13] M.C. Militello, S.J. Simko, Palladium oxide (PdO) by XPS, Surf. Sci. Spectra 3 (1994) 395–401.
[14] Y. Abe, K. Kato, M. Kawamura, K. Sasaki, Rhodium and rhodium oxide thin films characterized by XPS, Surf. Sci. Spectra 8 (2001) 117–125.
[15] G. Soldano, E.N. Schulz, D.R. Salinas, E. Santos, W. Schmickler, Hydrogen electrocatalysis on overlayers of rhodium over gold and palladium substrates—more active than platinum? Phys. Chem. Chem. Phys. 13 (2011) 16437–16443.